31 August 2001

ELSEVIER

Chemical Physics Letters 344 (2001) 565–572

CHEMICAL PHYSICS LETTERS

www.elsevier.com/locate/cplett

Saddle-node states in the spectra of HCO and DCO: a periodic orbit classification of vibrational levels

S. Stamatiadis [a], S.C. Farantos [a,*,1], Hans-Martin Keller [b], Reinhard Schinke [b]

[a] *Institute of Electronic Structure and Laser, Foundation for Research and Technology – Hellas, Iraklion, Crete 711 10, Greece*
[b] *Max-Planck-Institut für Strömungsforschung, Göttingen D-37073, Germany*

Received 29 May 2001; in final form 10 July 2001

Abstract

The general structures of the vibrational states of HCO and its isotopomer DCO are analyzed in terms of periodic orbits (POs) and continuation/bifurcation diagrams. Both bound and resonance states are considered. It is shown that the members of the pure overtones are guided by POs, even in the continuum. In particular, it is demonstrated that the highly anharmonic states localized along the dissociation coordinate correspond to orbits originating from saddle-node bifurcations in the classical phase space. © 2001 Elsevier Science B.V. All rights reserved.

1. Introduction

In two publications Keller et al. presented quantum mechanical calculations for bound as well as resonance states, that is quasi-bound states above the first dissociation threshold, for HCO [1] and DCO [2]. An analytical potential energy surface (PES) was used, which was constructed from accurate ab initio calculations [3]. The agreement of the calculated energies and resonance widths with data obtained from high resolution stimulated emission pumping (SEP) spectra [4,5] was excellent. For HCO, 15 bound states and 123 resonances were analyzed and the energy covered a range of ~2 eV above the H+CO threshold. For DCO, 29 bound states and about 140 resonances were investigated spanning an energy range of ~1.4 eV above threshold.

For HCO the coupling between the three internal degrees of freedom is comparably weak and therefore an assignment of the majority of the bound states as well as the resonance states in terms of three quantum numbers (v_1, v_2, v_3) is straightforward [1]; in what follows, v_1, v_2, and v_3 are the H(D)C stretch, the CO stretch and the bending quantum numbers, respectively. All three fundamental excitation energies for HCO are quite different so that resonance effects are basically not existing at lower energies. However, because the HC mode is – due to the shallow potential well of about 0.8 eV – strongly anharmonic, a 1:2 stretch:bend Fermi-type resonance, i.e., two quanta of the bending mode are roughly equal to one quantum of the HC mode, develops at higher energies and leads to considerable mixing [1].

For DCO, on the other hand, anharmonic mixings exist already for the lowest vibrational states [2,6,7] and become even stronger with increasing energy. The reason is an (accidental) 1:1:2

* Corresponding author. Fax: +30-81-39-1305.
E-mail address: farantos@iesl.forth.gr (S.C. Farantos).
[1] Also at Department of Chemistry, University of Crete, Iraklion 71110, Crete, Greece.

0009-2614/01/$ - see front matter
PII: S0009-2614(01)00832-6

resonance of the three fundamental frequencies: One quantum of DC stretch is worth one quantum of the CO stretch mode and two quanta of the bending mode. As a consequence, the majority of bound and resonance states cannot be clearly assigned in the usual sense by counting the nodes along the three coordinate axes; therefore, many of the assignments given in Table 1 in [2], based on projecting the exact wavefunctions on certain numerically defined zeroth-order wavefunctions, are rather vague. However, the wavefunctions shown in Fig. 11 of [2] are regular with recognizable nodal patterns, although not always along the normal coordinate directions.

Recently, Troellsch and Temps [8] have analyzed the bound and resonance states of DCO by using an effective polyad Hamiltonian. By introducing the inherent 1:1:2 multiple resonance among the three vibrational frequencies and fitting the parameters of the Hamiltonian to the experimental vibrational energies they were able to achieve good agreement with the observed levels and confirmed many of the assignments made before.

Understanding and assigning highly excited states of molecules – even if only three degrees of freedom are involved – is a general problem of molecular spectroscopy [9]. As energy increases the simple behavior usually found at low energies might change dramatically when particular effects like bifurcations, for example, arise [10]. However, applying tools developed in the last decades in nonlinear mechanics and employing semiclassical approximations are tremendously helpful in circumventing some of these problems. Particularly, the use of periodic orbits (POs) to explore the structure of the classical phase space over an extended energy range has been proved to be very valuable [11–13]. This approach has led to systematic studies of so-called *continuation/bifurcation* (C/B) diagrams of POs for a variety of molecules. The central conclusion of these studies is that families of POs offer an alternative way to assign spectra. HCP is an illuminating example for such an analysis [14].

In the present Letter we analyze the vibrational spectra of DCO and HCO in a similar fashion. The main structure of the classical phase space is revealed, and it is shown that the quantum mechanical vibrational states can be classified in terms of this structure.

2. PES and computational methods

The PES for the ground electronic state of HCO has been described in detail in [1]. The dynamics calculations are performed in terms of the Jacobi coordinates appropriate for the dissociation into H(D)+CO: R is the distance of H(D) from the center of mass of CO, r is the bond length of CO and γ is the angle between $\vec{R}$ and $\vec{r}$. The energy of the global minimum of the PES is −0.8339 eV and is located at $R = 3.0215\,a_0$, $r = 2.2325\,a_0$ and $\gamma = 144.86°$. The potential is zero for infinitely separated H(D) and CO with CO at equilibrium bond length. The dissociation barrier is 0.1254 eV and is located at $R = 4.2341\,a_0$, $r = 2.1489\,a_0$ and $\gamma = 131.94°$.

The classical Hamiltonian for zero total angular momentum reads

$$H = \frac{P_R^2}{2m_R} + \frac{P_r^2}{2m_r} + \left(\frac{1}{2m_R R^2} + \frac{1}{2m_r r^2}\right) P_\gamma^2 + V(R, r, \gamma), \tag{1}$$

where P_R, P_r and P_γ are the momenta conjugate to the Jacobi coordinates. The reduced masses are given by

$$m_R = \frac{(m_C + m_O)\, m_X}{m_C + m_O + m_X}, \quad m_r = \frac{m_C m_O}{m_C + m_O}, \tag{2}$$

where $m_X = m_H$ or m_D. Energies will be expressed in eV unless stated otherwise.

Details of how the periodic solutions for the classical equations of motion are computed and techniques for continuing these solutions in a parameter space have been described elsewhere [15]. To find the first PO for each family we exploit well-known existence theorems [16,17] of POs near the equilibria points of the potential function. Individual members of a family of POs are found by generalized Newton–Raphson multiple shooting methods [15]. The continuation of a family with energy leads to the construction of the C/B diagrams. After a PO is found its stability is analyzed,

which provides information about the character of nearby trajectories, i.e., whether it is stable or unstable.

3. Results and discussion

3.1. DCO

In constructing the continuation/bifurcation diagram, first the principal families of POs, i.e., those which start from the minimum of the potential, are located. During the continuation step several bifurcations are observed with the new POs having either the same period or multiples of the periods of the parent POs. In Fig. 1 we depict the C/B diagram for DCO. Shown are the frequencies of the POs ($2\pi\hbar/T$, where T is the period) as functions of the total energy, E. In order to keep the presentation clear, we show only the principal families ([SS], [AS] and [B]) and the first members of a series of saddle-node bifurcations ([SN1], [SN2], ...). They are sufficient for describing the main characteristics of the phase space structure and assigning the quantum mechanical overtone states. Saddle-node POs come into existence at critical energies and do not exist at lower energies. They have two branches: at the onset one branch corresponds to a stable PO whereas the other one consists of unstable POs.

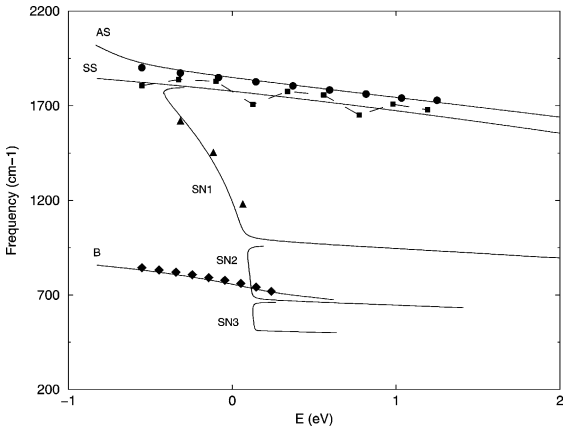

Fig. 1. Frequencies of the POs for the principal families and saddle-node bifurcations as functions of the total energy E in eVs (1 eV = 8065.541 cm^{-1}) for DCO. The symbols are the energy differences between neighboring quantum mechanical states (plotted with respect to the energy of the lower state) of the four progressions: circles $(1, v_2, 0)$, squares $(0, v_2, 0)$, triangles $(v_1, 0, 0)$ and diamonds $(0, 0, v_3)$. The dashed line connects the quantum levels of the SS overtone states (squares) to emphasize their oscillatory structure. See the text for more details.

Owing to the 1:1 stretch:stretch resonance the two stretch degrees of freedom are strongly mixed. As a consequence, the two POs which describe the stretching motion are neither parallel to R nor to r as clearly seen in Fig. 2, where in the first two columns examples of POs of the [AS] and [SS] types are shown for several energies. Since the two POs describe essentially symmetric and asymmetric stretching motions – especially at low energies, we will refer to the symmetric stretch (SS) and the asymmetric stretch (AS) families in what follows, despite the fact that the molecule has no distinct symmetry. The bending mode ([B]) can be clearly distinguished. The POs of the [AS] family remain stable up to the energy of 0.86 eV; at this value it undergoes a 'simple' bifurcation (POs with the same period emerge). The [SS] family is stable up to 0.75 eV where it undergoes a period-doubling bifurcation. A period-doubling bifurcation occurs for the [B] family at −0.077 eV, where the POs become single-unstable; a new period-doubling bifurcation takes place at 0.26 eV rendering the [B] family doubly unstable.

POs which represent dissociation come into existence at energies significantly above the minimum ($E = -0.418$ eV) in the first saddle-node bifurcation, [SN1]. Examples of POs belonging to the various [SN] families are depicted in the third column of Fig. 2. The initially stable branch of the [SN1] saddle-node bifurcation quickly becomes unstable and it shows several bifurcations as the energy increases. However, extended regions of stability were traced in its continuation with energy. Because the [SN] type orbits advance along the dissociation coordinate, their frequency rapidly decreases with increasing energy. It appears as if the [SN] POs are the extensions of the low-energy [AS] branch.

Included in the C/B diagram are the quantum mechanical transition frequencies of four pure progressions, which in the normal-mode terminology – appropriate for the lowest states – have the assignments: $(v_1, 0, 0)$, $(0, v_2, 0)$, $(1, v_2, 0)$ and

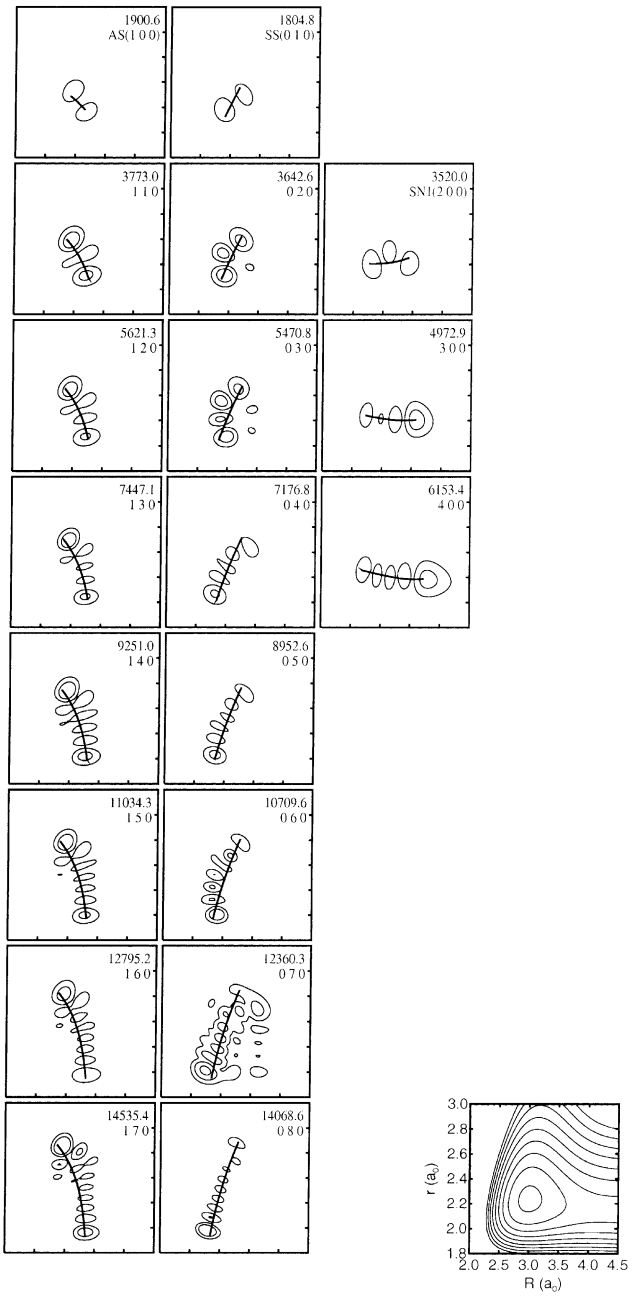

Fig. 2. Contour plots of the modulus square of eigenfunctions for DCO in the two stretch coordinates R and r. The lines superimposed on the contour lines are POs which characterize the eigenfunctions. The first column shows POs and wavefunctions of the [AS] type, the second column depicts POs and wavefunctions of the [SS] type and the third column contains orbits and wavefunctions of the [SN1] type. The first number in each panel is the transition energy (in cm^{-1}) with respect to the ground state and the second number is the normal-mode asignment according to [2]. For further details see the text. The corresponding two-dimensional potential is shown in the extra panel.

$(0,0,v_3)$. With pure progressions we mean states having wavefunctions with the maxima and minima aligned along a line without excitation in directions perpendicular to this line – like pearls on a necklace. Shown are the energy differences between adjacent levels of these progressions. This figure suggests that the bending states, $(0,0,v_3)$, correlate with the [B] POs, the $(0,v_2,0)$ states with the [SS] orbits and the $(1,v_2,0)$ states correspond to the [AS] POs. The states with excitation in the dissociation mode $(v_1,0,0)$ are clearly related to the [SN] POs (see Fig. 2).

These relations between the POs, on one hand, and the quantum mechanical states, on the other, are further substantiated by comparing the POs with the quantum mechanical wavefunctions (Fig. 2). Other examples of assignable eigenfunctions without excitation in the bending mode $(v_3 = 0)$ can be seen in Fig. 11 of [2]. In Fig. 2 the states are organized in terms of increasing polyad quantum number $P = v_1 + v_2 + v_3/2$. In each polyad there are $P + 1$ different states. A similar plot for a representative state with bending excitation is given in Fig. 3. There the contours of the wavefunctions are plotted in the (R,γ) plane. Also shown in Fig. 3 is the wavefunction for state $(2,0,0)$.

Figs. 1 and 2 together, beyond doubt, make clear that the states, which are characterized as DC stretch $(v_1,0,0)$, correspond to the saddle-node POs. Only the first level, $(1,0,0)$, must be attributed to the [AS] type of POs. At the energy of the next excited level, $(2,0,0)$, the saddle-node bifurcation [SN1] has appeared and marks the domains in phase space where eigenfunctions localized along the R coordinate can be found. The correspondence between the [SN] POs and the $(v_1,0,0)$ wavefunctions is particularly clear for the higher members. The highest level of this progression, $(4,0,0)$, lies just above the (classical) potential barrier to dissociation. Because of the direct excitation of the dissociation mode, the states $(5,0,0)$, $(6,0,0)$, etc. have very broad line widths and had not been identified in the quantum calculations [2]. Other regular and well localized eigenstates corresponding to the [SN] POs are shown in Fig. 11 of [2]. However, they do not further extend in the R direction but the additional energy is stored in the r coordinate. These states can be clearly assigned as $(4,1,0)$, $(4,2,0)$, etc.

According to the PO assignment the $(1,v_2,0)$ states should be labeled as [AS] states. Their assignment as $(1,v_2,0)$ in [2] was not made in view of the apparent nodal structure but with respect to a decomposition in terms of a set of basis functions. Table 1 in [2] clearly shows that the $(1,v_2,0)$ states are highly mixed. The $(0,v_2,0)$ states should be assigned as [SS] states. This correspondence is very clear for the highest members of this progression, but less obvious for the lower ones. That at lower energies the backbones of the $(0,v_2,0)$ states do not exactly follow the corresponding [SS] POs indicates significant mixing with other states. The small oscillations of the quantum mechanical frequencies of the [SS] states around the classical frequency very likely have the same origin.

3.2. HCO

As the three fundamental excitation energies are quite different, complications due to mixing effects are much less prominent for HCO than

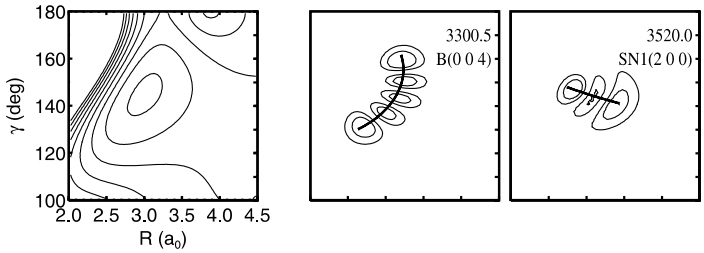

Fig. 3. The same as in Fig. 2 but the eigenfunctions are shown in the (R,γ) plane.

they are for DCO. As a consequence, all of the bound states and most of the resonance states can be readily assigned. Nevertheless, mixing effects are not completely absent and do affect some of the states. Two quanta of excitation in the bending mode (2139 cm^{-1}) are roughly worth one quantum of the HC stretch mode (2437 cm^{-1}). As a consequence, states with the same polyad quantum number $P = v_1 + v_3/2$ are grouped together in polyads, for the same CO stretch quantum number v_2. At lower energies the spacing between states within the same polyad is relatively large and mixing is weak. However, because the HC mode is very anharmonic, the spacing among the states decreases and the mixing becomes stronger. As a result, the wavefunctions for some states do not have an immediately apparent assignment (see below). Like for DCO, an analysis in terms of POs is helpful for understanding these subtleties.

Fig. 4 shows the C/B diagram of the principal families and saddle-node POs in the energy-frequency domain and Fig. 5 presents the contours of representative eigenfunctions in the (R, γ) plane with the POs superimposed. Additional plots of wavefunction can be found in Fig. 8 of [1]. All the states shown are without excitation in the r stretch. For HCO we denote the principal families of POs as [R] stretch, [r] stretch and [B] bend, because the orbits are clearly aligned along one of the three axes, at least at low energies.

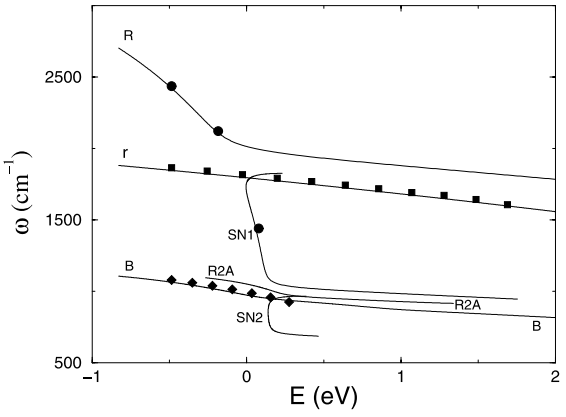

Fig. 4. Frequencies of the POs for the principal families and the saddle-node bifurcations as functions of the total energy E in eVs (1 eV = 8065.541 cm^{-1}) for HCO. The symbols are the energy differences between neighboring quantum mechanical states (plotted with respect to the energy of the lower state) of the three progressions: circles $(v_1, 0, 0)$, squares $(0, v_2, 0)$ and diamonds $(0, 0, v_3)$. See the text for more details.

The [R] family shows an early bifurcation with period-doubling at −0.26 eV where a new family, termed [R2A], appears. After this energy the [R] POs become single-unstable up to about 1.35 eV where they become stable again. Around 0.74 eV the [R2A] family becomes unstable through a simple bifurcation. The [r] family loses its stability with a period-doubling bifurcation at −0.12 eV. The [B] principal family becomes unstable in a period-doubling bifurcation at about −0.39 eV and completely unstable at 1.668 eV. The [SN1] appears just below the barrier to dissociation.

As can be seen in Fig. 4, at low energies the frequencies of the two stretch families and the bending family are well separated. However as the energy increases the anharmonicity of the potential along the dissociation mode causes the frequency of the [R] type POs to drastically decrease. It approaches the frequency of the [r] family or two times the frequency of the bending mode. The coupling between R and r is relatively weak so that these two modes do not interact appreciably. However, the coupling between R and γ is stronger leading to a profound 1:2 resonance condition. This leads to the period-doubling bifurcation and the birth of the [R2A] POs. The corresponding (curved) orbits in the lower row of Fig. 5 clearly illustrate the 1:2 resonance between R and γ. Just below the barrier to dissociation the [SN1] family emerges. The [SN] type POs are qualitatively similar to the [R] POs and therefore must be considered as their continuations to higher energies beyond the period-doubling bifurcation.

In Fig. 5 we can see that the bending overtones $(0, 0, v_3)$ are clearly marked by the POs of the [B] family. Likewise, the CO stretch overtone wavefunctions (not shown) clearly follow the [r] type POs. The first excited state in the R coordinate, $(1, 0, 0)$, is marked by an [R] type PO. However, the next state, $(2, 0, 0)$, shows a mixed

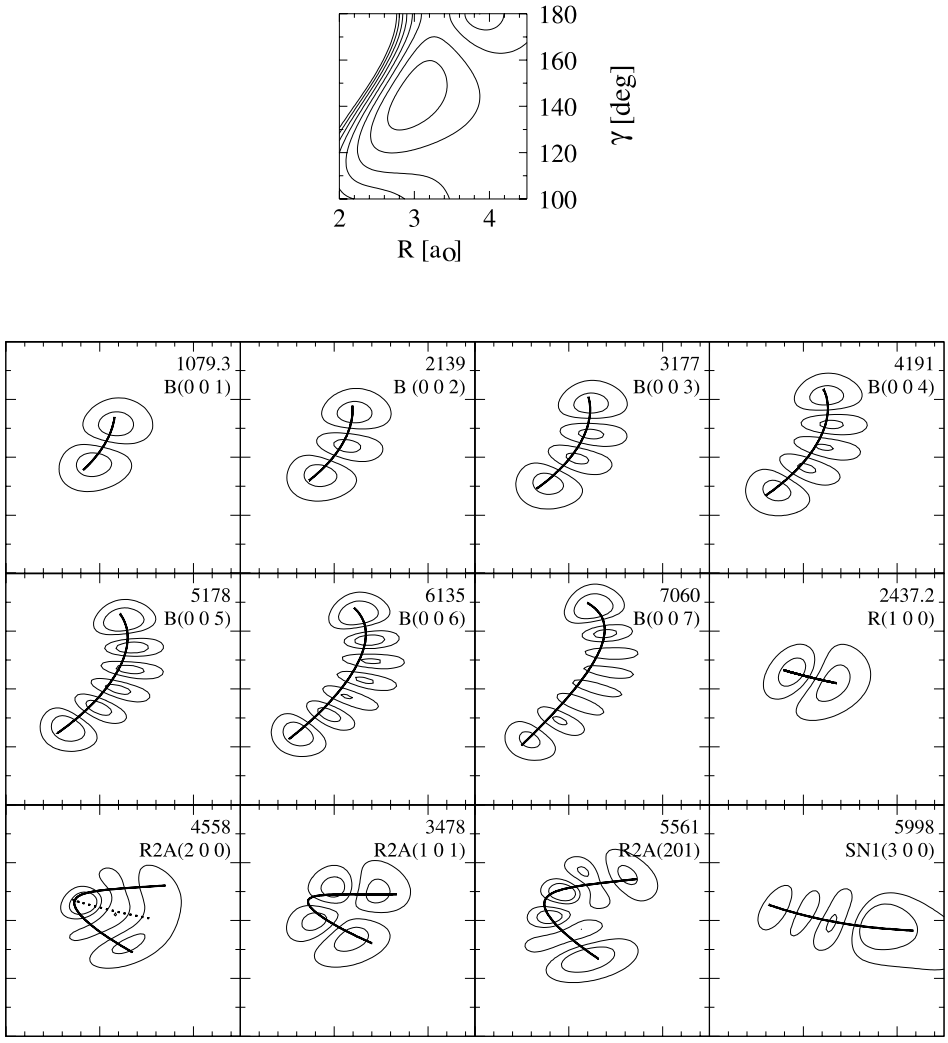

Fig. 5. Contour plots of the modulus square of eigenfunctions for HCO in the (R,γ) plane. The lines superimposed on the contour curves are POs which characterize the eigenfunctions. They are of the [B] type (panels 1–7), the [R] type (panel 8), the [R2A] type (panels 9–11), and the [SN1] type (panel 12). The first number in each panel is the transition energy (in cm^{-1}) with respect to the ground state and the second number is the normal-mode asignment according to [1]. For further details see the text. The corresponding two-dimensional potential is shown in the extra panel.

character of [R] and [R2A] POs. The well-localized $(3,0,0)$ state is due to the penetration of this state in the domain of the [SN1] type POs. Finally, the [R2A] POs are the backbones of states like $(1,0,1)$, $(2,0,1)$ and $(1,0,4)$ (the latter is shown in Fig. 8 of [1]). Because the states with higher excitation in the dissociation mode are very short-lived, they have not been identified in [1].

4. Conclusions

In this Letter a PO analysis and a classification of the vibrational overtone levels of DCO and HCO have been presented. Establishing relations between POs, on one hand, and quantum mechanical energy levels, on the other, not only provides an assignment, which is free of the coordinate system used, but also reveals details of the dynamical

behavior in regions of the phase space where the dynamics is dominated by resonances. Assignments in terms of POs often are more meaningful than assignments in terms of normal mode quantum numbers. The most interesting observation is the existence of saddle-node bifurcations in the classical phase space, which leads to the birth of a new progression at energies well above the global minimum. As a consequence, there are four instead of three overtone progressions.

This behavior is somehow reminiscent of HOCl and HCP. In HOCl, POs which at low energies advance along the dissociation coordinate at higher energies change their behavior and avoid the dissociation channel. POs advancing along the fragmentation coordinate come into existence at a saddle-node bifurcation [18,19]. In HCP a similar behavior is observed for the bending coordinate [14]. In both cases there is a 1:2 resonance between the bending and one of the stretches. In DCO, there is a 1:1 resonance between the two stretch modes. In all these examples one of the critical modes involved in the resonance is the 'reaction' coordinate – the dissociation coordinate in HOCl and DCO or the isomerization coordinate in HCP.

Locating POs in systems with more than two degrees of freedom is, due to the existence of different sorts of bifurcations, a complicated task. However, the present study as well as previous ones on triatomic systems demonstrates that finding the principal families and a few bifurcations with low multiplicity is sufficient to reveal the main topological characteristics of the eigenfunctions and to understand the spectrum over wide ranges of energies.

Saddle-node states are characteristic features of all nonlinear systems, including strongly bound molecules. DCO and HCO are two more examples for which they have been seen in experimental spectra. HCP was the first molecule for which [SN] states have been identified in a measured spectrum [20].

Acknowledgements

S.C.F and R.S. are pleased to acknowledge financial support from the Alexander von Humboldt–Stiftung.

References

[1] H.-M. Keller, H. Flöthmann, A.J. Dobbyn, R. Schinke, H.-J. Werner, C. Bauer, P. Rosmus, J. Chem. Phys. 105 (1996) 4983.
[2] H.-M. Keller, T. Schröder, M. Stumpf, C. Stöck, F. Temps, R. Schinke, H.-J. Werner, C. Bauer, P. Rosmus, J. Chem. Phys. 106 (1997) 5359.
[3] H.-J. Werner, C. Bauer, P. Rosmus, H.-M. Keller, M. Stumpf, R. Schinke, J. Chem. Phys. 102 (1995) 3593.
[4] J.D. Tobiason, J.R. Dunlop, E.A. Rohlfing, J. Chem. Phys. 103 (1995) 1448.
[5] C. Stöck, X. Li, H.-M. Keller, R. Schinke, F. Temps, J. Chem. Phys. 106 (1997) 5333.
[6] R.N. Dixon, Trans. Faraday Soc. 564 (1969) 3141.
[7] J.M. Bowman, J.S. Bittman, L.B. Harding, J. Chem. Phys. 85 (1986) 911.
[8] A. Troellsch, F. Temps, Z. Phys. Chem. 215 (2001) 207.
[9] H.-L. Dai, R.W. Field (Eds.), Molecular Dynamics and Spectroscopy by Stimulated Emission Pumping, World Scientific, Singapore, 1995.
[10] M.C. Gutzwiller, Chaos in Classical and Quantum Mechanics, Springer, New York, 1990.
[11] J.M. Gomez Llorente, E. Pollak, Ann. Rev. Phys. Chem. 43 (1992) 91.
[12] S.C. Farantos, Int. Rev. Phys. Chem. 15 (1996) 345.
[13] M.E. Kellman, in: H.-L. Dai, R.W. Field (Eds.), Molecular Dynamics and Spectroscopy by Stimulated Emission Pumping, World Scientific, Singapore, 1995.
[14] H. Ishikawa, R.W. Field, S.C. Farantos, M. Joyeux, J. Koput, C. Beck, R. Schinke, Ann. Rev. Phys. Chem. 50 (1999) 443.
[15] S.C. Farantos, Comp. Phys. Commun. 108 (1998) 240.
[16] A. Weinstein, Inv. Math. 20 (1973) 47.
[17] J. Moser, Commun. Pure Appl. Math. 29 (1976) 727.
[18] R. Jost, M. Joyeux, S. Skokov, J.M. Bowman, J. Chem. Phys. 111 (1999) 6807.
[19] J. Weiß, J. Hauschildt, S.Yu. Grebenshchikov, R. Düren, R. Schinke, J. Koput, S. Stamatiadis, S.C. Farantos, J. Chem. Phys. 112 (2000) 77.
[20] H. Ishikawa, C. Nagao, N. Mikami, R.W. Field, J. Chem. Phys. 106 (1997) 2980.